Numerical optimization of ultrasound transducers by the linearity of the phase spectrum

K. K. Andersen, M. Frijlink and L. Hoff

Submitted version of article in
IEEE International Ultrasonics Symposium (IUS)

Publisher's version: K. K. Andersen, M. Frijlink and L. Hoff, "Numerical optimization of ultrasound transducers by the linearity of the phase spectrum," *2017 IEEE International Ultrasonics Symposium (IUS)*, Washington, DC, 2017, pp. 1-1.
doi: 10.1109/ULTSYM.2017.8092613

Numerical Optimization of Ultrasound Transducers by the Linearity of the Phase Spectrum

Kenneth K. Andersen*†, Martijn Frijlink*, Lars Hoff*
*Department of Microsystems
University College of Southeast Norway
Horten, Norway
†Email: Kenneth.Andersen@usn.no

***Abstract*—New ultrasound imaging and therapeutic modalities may require transducer designs that are not easily facilitated by conventional design guidelines and analytical expressions. This motivates the investigation of numerical optimization methods that can include the effect of structural layers (e.g. bonding and electrodes), electrical loading, and more than one active piezoceramic layer in the design and optimization procedure. We have developed a numerical design method that utilizes the linearity of the spectral phase as the design criterion. The aim of this paper is to apply our numerical optimization method to optimize a transducer by linearizing the phase spectrum. Comparison to an established, analytical, broad-band matching method is given.**

I. Introduction

Ultrasound imaging transducers are typically designed to have bandwidths larger than e.g. 60% to achieve the desired short pulse duration for high axial resolution. However, if the transducer's spectrum contains sharp transitions at the band edges, this can lead to so-called time-sidelobes in the impulse response. If the time-sidelobe level is high relative to the main lobe, image degradation may occur [1, p. 122]. Typically a lossy material is attached to the back of the transducer which may smoothen the band edges of the spectrum and reduce such tails. However, this also leads to an unwanted reduction in the transducer's sensitivity. Preferably, the backing material has a low characteristic impedance, and air-backed transducers are for those reasons, an important class of transducers.

Since the objective of an imaging transducer is to transmit short pulses, and not necessarily exhibit a wide bandwidth, we focus on a transducer criteria that is directly related to the length of the transmitted pulse, i.e. the phase spectrum. Pohlig [2] has shown that for a given spectrum the shortest impulse response is obtained if the spectrum has a linear phase. Applied to ultrasound imaging transducers, this means that the shortest pulses are obtained when the transducer is designed to have a linear phase in the relevant frequency band.

Based on this, we have developed a numerical optimization method for ultrasound transducers by linearizing the phase spectrum. The optimization is performed by repeated 1D simulations of a transducer structure where a selected set of transducer parameters are changed stochastically. The optimal transducer is obtained by the Simulated Annealing algorithm [3]. Although several numerical optimization methods have been proposed [4]–[6], to the authors knowledge, no one has yet used the phase spectrum as an optimization criterion.

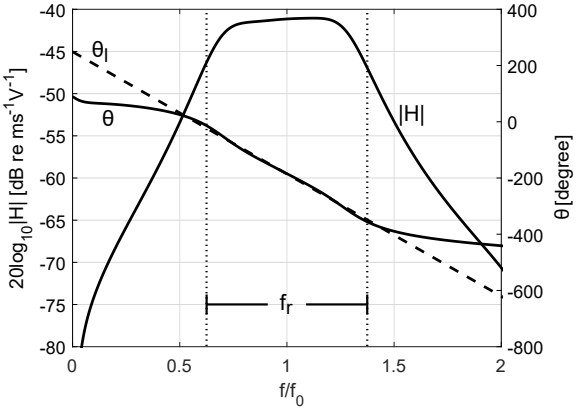

Fig. 1. A typical spectrum of the transmit transfer function $H(\omega) = U(\omega)/V(\omega)$ is shown, where U is the complex particle velocity at the face of the transducer, V is the complex input voltage at the terminals of the transducer, and $\omega = 2\pi f$ is angular frequency. $|H|$ denotes magnitude (solid) and θ denotes phase spectrum (solid). The fitting range is indicated by f_r and the ideal linear phase θ_l (dashed) is also shown.

To demonstrate the linear phase method, we optimize the matching section of a simulated air-backed piezoceramic transducer with two matching layers. We compare the optimized transducer with a similar transducer where the matching section is defined using the established, analytical, broad-band matching equations derived by Desilets [7].

II. Optimization method

A. Linear phase spectrum

A typical spectrum of a transmitter transfer function $H(\omega) = U(\omega)/V(\omega)$ is shown in Fig. 1, where U is the complex normal particle velocity at the face of the transducer, V is the complex input voltage at the terminals of the transducer, $\omega = 2\pi f$ is the angular frequency, and $H = |H|\exp(i\theta)$, where $|H|$ denotes magnitude and θ is the spectral phase. The transducer's spectral phase, $\theta = \theta(\bar{x})$, is a function of all physical parameters that describes the transducer, where $\bar{x} = x_1, x_2, \ldots, x_j$ is a vector containing all the transducer parameters.

To quantify the linearity of the spectral phase a regression line is fitted to the spectral phase over a frequency range $[f_{min}, f_{max}]$, denoted *fitting range*, i.e.

$$\theta_l = \beta_0 + f\beta_1, \quad f \in [f_{min}, f_{max}], \tag{1}$$

where θ_l is referred to as an ideal linear phase, f is frequency, and β_0 and β_1 are the coefficients of the regression line. The coefficients β_0 and β_1 are obtained from linear regression using Matlab (The MathWorks, Inc., Natick, Mass., USA).

The approach is to search the parameter space $\bar{x}$ that minimize the difference between the ideal linear phase, θ_l, and the transducer phase, θ, mathematically expressed as

$$\arg\min_{\bar{x}} E(\bar{x}), \tag{2}$$

where $E(\bar{x})$ is referred to as the cost function to be minimized, and is defined as

$$E(\bar{x}) = \frac{1}{m}\sqrt{\sum_{i=1}^{m}[\theta(f_i,\bar{x}) - \theta_l(f_i,\bar{x})]^2}, \quad f_i \in [f_{min}, f_{max}], \tag{3}$$

where $E = E(\bar{x})$ is the average absolute difference between the ideal linear phase $\theta_l(f_i, \bar{x})$ and the simulated transducer's spectral phase $\theta(f_i, \bar{x})$ summed over m discrete frequency points in the fitting range $[f_{min}, f_{max}]$.

B. Simulation and optimization set-up

As an example of the linear phase method, the acoustic matching section of a simulated air-backed piezoceramic transducer with center frequency $f_0 = 4$ MHz will be optimized accordingly. A schematic of the transducer stack is shown in Fig. 2. The transducer consists of a $\lambda/2$-thick piezoceramic layer with 12 μm silver electrodes, two matching layers and 3 μm bondlines mechanically connecting the layers. The transducer is radiating in water.

The transducer is simulated by a 1D equivalent circuit model suggested by Mason [8], implemented as an admittance matrix. The Mason model is well established for piezoelectric transducer structures oscillating in thickness mode, however if other oscillation modes are present, other models should be considered, e.g. a finite element method.

For our example, we have used the material parameters for a common piezoceramic Ferroperm™ Pz27 (Meggitt Sensing Systems, Denmark) provided by the manufacturer. The remaining material parameters are realistic.

The transducer parameters we are optimizing are the characteristic impedance, Z_n, and the thickness, l_n, for each matching layer n, represented as two dimensionless ratios Z_n/Z_p and l_n/λ_n, where Z_p denotes the characteristic impedance in the piezoceramic plate and λ_n denotes the wavelength in the n'th matching layer. In our case, this leads to four optimization parameters,

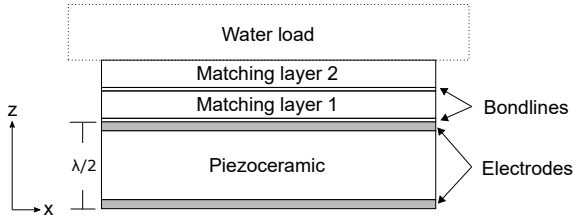

Fig. 2. Schematic of the transducer structure.

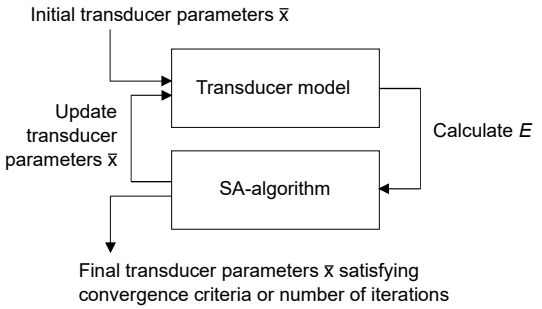

Fig. 3. Schematic of the optimization procedure. $\bar{x} = x_1, x_2, ...x_j$ are the physical transducer parameters and E is the cost function to be minimized. In the current work, the 1D model of Mason is used to simulate the transducer and the Simulated Annealing algorithm is used to obtain the optimal transducer.

$$\left\{\frac{Z_1}{Z_p}, \frac{l_1}{\lambda_1}, \frac{Z_2}{Z_p}, \frac{l_2}{\lambda_2}\right\}. \tag{4}$$

The optimization is done by stochastically varying the ratios Z_n/Z_p and l_n/λ_n and updating the transducer parameter vector, $\bar{x}$, with the new parameter values. The optimal transducer is obtained using the Simulated Annealing algorithm [3] implementation in MATLAB's *Optimization Toolbox*, Release 2016a. See Fig. 3 for a schematic of the optimization process. The optimization process is initiated using a set of transducer parameter values, $\bar{x}$, either generated randomly or based on an established model, e.g. Desilets [7]. Bounds on $\bar{x}$ may be applied to minimize the search; e.g., in the current work, the upper bounds on l/λ was half a wavelength. The optimization process finishes when a set convergence criteria is met, or when a set iteration limit is reached.

III. Results

The linear phase method was used to optimize the acoustic matching section of the transducer in Fig. 2. The fitting range was 2.7 MHz to 5.3 MHz, corresponding to a 65% relative bandwidth. The results are compared to a similar transducer, where the matching section was defined using the established, analytical equations derived by Desilets [7].

The optimized values are given in Table I. The characteristic impedance in matching layer 1 obtained by the linear phase method is 16.7% lower than what is obtained using Desilets' equations, while for matching layer 2 a 3% lower value is obtained. The thickness l of the matching layers are in Desilets' model fixed to $\lambda/4$, however, since the added mass of

TABLE I
OPTIMIZATION RESULTS

Matching layer	Desilets		Linear phase	
	Z [MRayl]	l/λ	Z [MRayl]	l/λ
1	8.83	0.242	7.36	0.249
2	2.34	1/4	2.27	0.256

the silver electrodes are not accounted for it was necessary to reduce the thickness of matching layer 1 by 3.6% to preserve a flat magnitude spectrum. When optimizing for a linear phase, we obtained approximately a $\lambda/4$-thickness for matching layer 1, and for matching layer 2, a 2.4% increase from a $\lambda/4$-thickness was obtained.

Simulated spectra and pulse shapes for the two transducers using the optimized values in Table I are shown in Fig. 4 (a–d). The black curves correspond to the results obtained using the linear phase method, and the red curves correspond to the results obtained using Desilets' equations.

In Fig. 4 (a) the two magnitude spectra exhibit a fundamental difference: the spectrum obtained with the linear phase method resembles a Gaussian, while the spectrum obtained by Desilets' equations exhibits a nearly flat top. The -3 dB bandwidths are 48.3% and 62.5%, for the linear phase method and Desilets' equations, respectively.

The two phase spectra in Fig. 4 (a) look very similar and both show a close to linear variation with frequency over the fitting range. To distinguish the variations in the phase spectra, the group delay, $-\partial\theta/\partial\omega$, of the two phases is shown in Fig. 4 (b). The constant group delay of an ideal linear phase is shown for comparison. This plot of the group delay highlights the difference between the two approaches. The passband ripple obtained with the linear phase method is -0.75 dB, while the passband ripple obtained by Desilets' equations is -3.6 dB. Outside of this frequency range, the difference is negligible.

In Fig. 4 (c) the impulse responses of the simulated spectra are given. Until about 0.5 μs, no significant difference between the two methods is observed. Beyond this, the impulse response corresponding to the linear phase method exhibits less and monotonically ringing at the expense of a slightly wider main lobe.

To illustrate and quantify this difference, the envelope of the two impulse responses is shown in Fig. 4 (d). The envelope $e(t)$ is defined as the magnitude of the analytic signal, calculated from the Hilbert transform. The highest time-sidelobe level obtained by the linear phase method is -29.4 dB, while Desilets' equations gives a time-sidelobe level at -16.6 dB.

IV. DISCUSSION

In the results section we saw that optimizing for a linear phase versus Desilets' equations gave a reduction in the bandwidth (48.3% compared to 62.5%, respectively) and a widening of the main lobe of the impulse response, however, a significant reduction in the time-sidelobe level was also seen (cf. Fig 4 (d)). As mentioned in the introduction, if the time-sidelobe levels are high relative to the main lobe, image degradation may occur, especially if the time-sidelobes do not decay monotonically.

From this we learn that optimizing for a wide-banded transducer is not necessarily the best and, at least, not the only approach for an imaging transducer, and we note that bandwidth as a quantitative measure for imaging transducers may be misleading.

A quantitative measure for imaging transducer that is used, is the width of the analytic envelope of the impulse response at e.g. -6 dB or -20 dB. However, from Fig. 4 (d) we see that the choice of decibel level will alter the result significantly. For example, at -6 dB the impulse response obtained with Desilets' equations is 4.1% shorter than what is obtained with the linear phase method; and at -20 dB the impulse response obtained with the linear phase method is 31% shorter than what is obtained with Desilets' equations. A discrepancy stemming from the choice of decibel levels are, off course, unwanted.

To aid in quantifying the performance of different transducers we propose that the average deviation from an ideal linear phase, E as defined in Eq.(3), over a stated bandwidth may be used as a quantitative measure for imaging transducers. For example, at the respective -3 dB bandwidths, E is 0.01° and 0.09° for the linear phase method and Desilets' equations respectively.

Desilets' equations do not take into account the effect of structural layers, such as finite electrode thickness, bonding layers or electrical connection, however, it is well known that this may affect the overall performance of an ultrasound transducer. The linear phase method permits the inclusion of such structural layers in the solution. In Fig. 5 an example of this is shown. Here we show the resulting thicknesses for matching layer 1 and 2 obtained by the linear phase method as a function of varying the thickness of the silver electrode from 0 to 20 μm. The impedance of both matching layers were held constant using the values in Tab. I. The linear phase method obtains a close to linear variation in the thickness of both matching layers with electrode thickness.

V. CONCLUSION

A numerical design method for ultrasound transducers utilizing the linearity of the spectral phase has been presented. Simulation results demonstrated an implementation of the method. We found that a transducer optimized for a linear phase resulted in a transducer with an impulse response with less and monotonically ringing compared to a transducer optimized using the established broad-band matching equations derived by Desilets.

Most importantly, the linear phase method can be used to optimize transducers with more complex structures than the presented example. Specifically, it allows for structural layers (e.g. backing, bonding, electrodes), electrical loading, and more than one active piezoceramic layer to be included in the design and optimization procedure, which is not trivial using the existing analytical methods.

Therefore, we believe that the linear phase method can be a valuable design method for medical transducers, both for con-

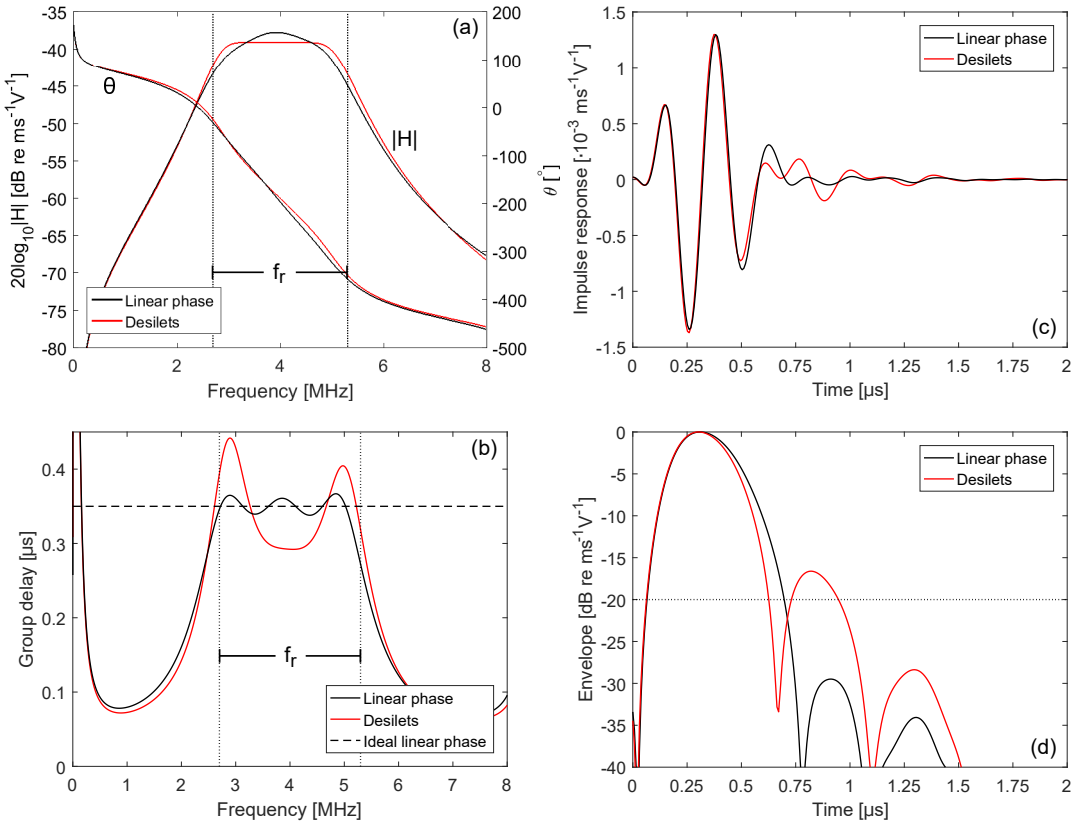

Fig. 4. Optimization results for the linear phase method (black) compared to the analytical equations derived by Desilets [7] (red). (a) Magnitude $|H|$ and phase θ of the transmit transfer function H. (b) Group delay, $-\partial\theta/\partial\omega$, of the two phases in (a). The constant group delay of an ideal linear phase is shown for comparison. (c) Impulse response, $h = F^{-1}\{H\}$, where F^{-1} denotes the inverse Fourier transform. (d) Normalized magnitude of the analytic signal, denoted envelope, $e(t)$, of the impulse responses in (c). The vertical line marks the -20 dB level. Where applicable, f_r indicates the frequency range where the cost function E was calculated.

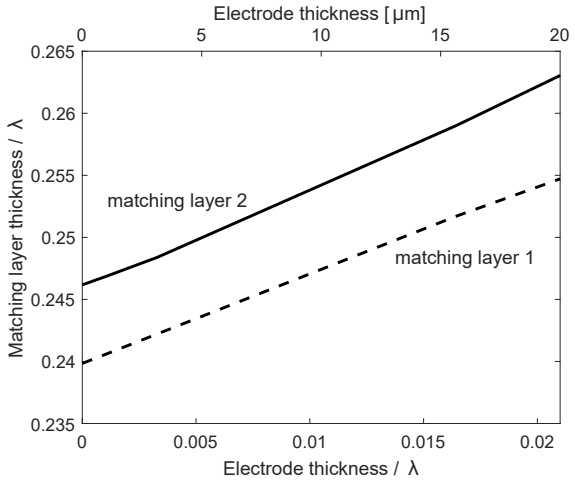

Fig. 5. Effect of the thickness of the silver electrodes on the thickness of the matching layers relative to the wavelength, λ.

ventional imaging transducers, and more complex transducers that are designed for new imaging and therapeutic modalities.

ACKNOWLEDGMENT

This work was supported by the Research Council of Norway (grant number 237887).

REFERENCES

[1] T. L. Szabo, *Diagnostic ultrasound imaging: Inside out*, 1st ed. Elsevier Academic Press, 2004.

[2] S. C. Pohlig, "Signal duration and the Fourier transform," *Proceedings of the IEEE*, vol. 68, no. 5, pp. 629–630, May 1980.

[3] S. Kirkpatrick, C. D. Gelatt, Jr, and M. P. Vecchi, "Optimization by simmulated annealing," *Science*, vol. 220, no. 4598, pp. 671–680, 1983.

[4] A. R. Selfridge, R. Baer, B. T. Khuri-Yakub, and G. S. Kino, "Computer-Optimized Design of Quarter-Wave Acoustic Matching and Electrical Matching Networks for Acoustic Transducers," in *1981 Ultrasonics Symposium*, Oct. 1981, pp. 644–648.

[5] J. M. Thijssen, W. A. Verhoef, and M. J. Cloostermans, "Optimization of ultrasonic transducers," *Ultrasonics*, vol. 23, no. 1, pp. 41–46, 1985. [Online]. Available: http://www.sciencedirect.com/science/article/pii/0041624X85900095

[6] T. L. Rhyne, "Computer optimization of transducer transfer functions using constraints on bandwidth, ripple, and loss," *IEEE Transactions on Ultrasonics, Ferroelectrics, and Frequency Control*, vol. 43, no. 6, pp. 1136–1149, Nov. 1996.

[7] C. S. Desilets, J. D. Fraser, and G. S. Kino, "The design of efficient broad-band piezoelectric transducers," *IEEE Transactions on Sonics and Ultrasonics*, vol. 25, no. 3, pp. 115–125, May 1978.

[8] W. P. Mason, *Electromechanical transducers and wave filters*. Princeton, NJ, Van Nostrand, 1948.